Experimental and Computational Investigations of the Reaction of OH with CF_3I and the Enthalpy of Formation of HOI

R. J. Berry,*,† Jessie Yuan,‡,§ Ashutosh Misra,‡,|| and Paul Marshall*,†,‡

Center for Computational Modeling of Nonstructural Materials, Air Force Research Laboratory, Materials Directorate, Wright-Patterson Air Force Base, Ohio 45433, and Department of Chemistry, University of North Texas, P.O. Box 305070, Denton, Texas 76203

Received: January 6, 1998; In Final Form: April 29, 1998

The kinetics of the reaction of hydroxyl radicals with trifluoroiodomethane were investigated by the flash photolysis−resonance fluorescence technique. A rate constant of $k = 5.8 \times 10^{-12} \exp((-11.3 \text{ kJ mol}^{-1})/RT)$ cm^3 molecule^{-1} s^{-1} was measured over the temperature range 280−450 K with accuracy limits of 20% (450 K) to 30% (280 K). Different product channels were investigated by ab initio methods, and the dominant products are CF_3 + HOI. The enthalpy of formation of hypoiodous acid was analyzed with Gaussian-2 theory, in conjunction with G2 energies for INO, ICN, ClCN, and other species. The transition state and reaction coordinate for OH + CF_3I was characterized at the G2(MP2) level, and the results suggest a negligible barrier to the reverse reaction of CF_3 + HOI, so that the measured forward activation energy can be used to derive $\Delta_f H_{298}(\text{HOI}) = -69.6 \pm 5.4$ kJ mol^{-1}. The implications of the kinetics and thermochemistry for iodine chemistry in flames and the atmosphere are discussed, and for the range 280−2000 K a proposed rate expression is $k = 2.9 \times 10^{-16}(T/\text{K})^{1.5} \exp(-(960 \text{ K})/T)$ cm^3 molecule^{-1} s^{-1}.

1. Introduction

Trifluoroiodomethane is a possible replacement for Halon-1301 (CF_3Br) as a fire suppression agent in some applications,[1] following the ban on Halon production under the Montreal Protocol on Substances that Deplete the Ozone Layer. A potentially important step in the combustion chemistry of CF_3I is the reaction

$$\text{OH} + \text{CF}_3\text{I} \rightarrow \text{CF}_3 + \text{HOI} \qquad (1)$$

whose kinetics have been investigated previously only at room temperature.[2,3] The two earlier studies yielded rate constants k_1 that differ by a factor of 4. One aim of the present work is to determine the Arrhenius parameters of the isolated elementary reaction for the first time, to permit estimation of k_1 at flame temperatures. The second aim is to measure k_1 at below room temperature, to assess the atmospheric lifetime of CF_3I at the average tropospheric temperature of around 280 K. The third aim is to assess the main products of the reaction. Finally, the kinetic measurements are combined with ab initio information about the potential energy surface to obtain the thermochemistry of a dominant product, hypoiodous acid. HOI is a major product of the reaction of ground-state atomic oxygen with C_2H_5I and larger iodoalkanes[4,5] and recently has been studied by photoionization[6] and FT-IR emission techniques.[7] $\Delta_f H_{298}$(HOI) has not previously been determined experimentally, despite its importance in understanding the photodissociation dynamics[8] and photoionization[6] of hypohalous acids and the roles of HOI in the mechanisms of iodine-mediated flame suppression[9] and stratospheric iodine chemistry.[10] Here we employ an ab initio potential energy surface (PES) to estimate the activation energy for the reverse rate constant k_{-1} and thus obtain the thermochemistry of reaction 1. The result is checked against results from Gaussian-2 (G2) theory, which for first- and second-row elements has a typical accuracy of about 8 kJ mol^{-1}.[11]

2. Experimental Method

The gas-handling system and the flash photolysis−resonance fluorescence reactor are described elsewhere.[12−14] Briefly, OH radicals were generated by flash lamp photolysis of water vapor through magnesium fluoride optics ($\lambda > 120$ nm), in the presence of excess CF_3I in a buffer of Ar gas. The CF_3I (Aldrich 99%) was purified by freeze−pump−thaw cycles at 77 and 190 K. [OH] was monitored as a function of time by resonance fluorescence at $\lambda \approx 307$ nm, excited from a flow of 2% H_2O vapor in Ar through a microwave-powered discharge lamp, and isolated with a band-pass filter before detection by a photomultiplier tube with photon-counting electronics. The signals I_f from typically 100−500 pulses were averaged before analysis by nonlinear least-squares fitting to an exponential decay plus a steady background B from scattered resonance radiation:[15]

$$I_f = A \exp(-k_{ps1}t) + B \qquad (2)$$

where the pseudo-first-order decay coefficient is

$$k_{ps1} = k_{1,\text{eff}}[\text{CF}_3\text{I}] + k_{\text{diff}} \qquad (3)$$

k_{diff} describes the first-order loss of OH by diffusion to the walls of the reactor and was typically 50−150 s^{-1}. The effective second-order rate constant $k_{1,\text{eff}}$ was obtained from the slope of plots of typically four to six k_{ps1} values vs [CF_3I] from 0 to

† Materials Directorate.
‡ University of North Texas.
§ Present address: Texas Instruments, Inc.,13553 Floyd Rd, MS 374, Dallas, TX 75265.
|| Present address: Air Liquide Electronics Chemicals & Services, Inc., 13546 North Central Expressway, MS 301, Dallas, TX 75243.

S1089-5639(98)00645-8 CCC: $15.00
Published on Web 06/11/1998

TABLE 1: Summary of Experimental Measurements for the Reaction CF_3I + OH

T, K	P, mbar	τ_{res}, s	F, J	$[H_2O]$, 10^{15} cm^{-3}	$[CF_3I]_{max}$,[a] 10^{14} cm^{-3}	$k_{1,eff} \pm \sigma_{k1,eff}$, 10^{-13} cm^3 molecule^{-1} s^{-1}
281	68.2	1.6	5.00	3.8	12.1	1.96 ± 0.14
281	54.1	1.0	5.00	2.3	8.8	1.74 ± 0.04
281	89.8	1.7	5.00	3.1	10.9	1.67 ± 0.06
281	68.2	1.6	4.05	3.8	12.1	1.71 ± 0.10
281	54.1	1.0	4.05	2.3	8.8	1.52 ± 0.05
281	89.8	1.7	4.05	3.1	10.9	1.29 ± 0.08
281	68.2	1.6	2.50	3.8	10.0	1.25 ± 0.09
281	54.1	1.0	2.50	2.3	8.8	1.01 ± 0.06
281	89.8	1.7	2.50	3.1	10.9	1.07 ± 0.06
281						*0.43 ± 0.14*[b]
292	75.2	1.7	5.00	2.8	17.8	1.39 ± 0.10
292	75.3	1.7	5.00	2.2	13.9	2.18 ± 0.15
292	71.0	1.6	5.00	4.0	12.7	2.10 ± 0.09
292	63.9	1.4	5.00	3.3	15.6	1.59 ± 0.13
292	68.0	1.5	4.05	2.6	22.1	1.48 ± 0.06
292	59.1	1.0	4.05	1.7	16.9	1.44 ± 0.05
292	71.1	1.6	4.05	2.8	14.3	1.88 ± 0.13
292	72.1	1.6	4.05	4.7	13.5	1.90 ± 0.12
292	75.2	1.7	2.50	2.8	17.9	1.26 ± 0.07
292	69.6	1.6	2.50	2.6	16.3	1.16 ± 0.08
292	64.0	1.4	2.50	3.3	15.2	1.20 ± 0.04
292	62.7	1.5	2.50	2.3	14.9	1.17 ± 0.02
292						*0.59 ± 0.14*[b]
338	83.2	1.6	5.00	2.6	12.3	2.23 ± 0.13
335	67.5	1.1	5.00	2.0	8.5	2.21 ± 0.11
338	115.7	2.3	4.05	4.3	16.2	2.18 ± 0.12
338	76.5	1.1	4.05	2.2	9.5	1.77 ± 0.09
338	83.2	1.6	4.05	2.6	12.3	2.11 ± 0.15
338	83.2	1.6	2.50	2.6	12.3	1.84 ± 0.13
335	67.5	1.1	2.50	2.0	8.5	1.49 ± 0.08
337						*0.96 ± 0.27*[b]
391	100.6	1.7	5.00	3.4	11.4	3.38 ± 0.19
390	68.5	1.0	5.00	2.1	6.9	3.03 ± 0.14
391	100.6	1.7	4.05	3.4	11.4	2.55 ± 0.30
390	68.5	1.0	4.05	2.1	6.9	2.69 ± 0.07
391	100.6	1.7	2.50	3.4	11.4	2.52 ± 0.18
390	68.5	1.0	2.50	2.1	6.9	2.26 ± 0.17
391						*1.56 ± 0.34*[b]
445	92.0	1.3	5.00	3.0	2.0	7.06 ± 0.27
443	89.0	1.8	5.00	3.4	8.1	4.95 ± 0.18
442	59.5	1.2	5.00	2.4	7.0	4.41 ± 0.13
445	92.0	1.3	4.05	3.0	2.0	6.45 ± 0.55
443	89.0	1.8	4.05	3.4	8.1	4.34 ± 0.17
442	59.5	1.2	4.05	2.4	7.0	3.94 ± 0.18
445	92.0	1.3	2.50	3.0	2.0	4.48 ± 0.17
443	89.0	1.8	2.50	3.4	6.0	3.92 ± 0.23
442	59.5	1.2	2.50	2.4	7.0	3.64 ± 0.19
443						3.15 ± 0.98[b]

[a] Typical lowest nonzero value of $[CF_3I] \approx 0.2[CF_3I]_{max}$. [b] Numbers in italics are the linear extrapolations of $k_{1,eff}$ to zero flash energy for each temperature and 1σ uncertainty of the intercept, from fits to the sets of $k_{1,eff}$ at each temperature.

$[CF_3I]_{max}$. The glass reactor was modified from that employed to investigate OH + silane reactions[14] by the addition of heating tape to reach elevated temperatures, up to about 450 K, and by the use of an ice bath to lower the temperature to about 280 K. The gas temperature at the reactor center was measured at the beginning and end of each experimental run with a moveable chromel−alumel thermocouple, calibrated against melting ice and boiling water. At each temperature studied various experimental parameters were varied to see how they influenced $k_{1,eff}$. These included the total pressure P and average gas velocity, which determine the average gas residence time in the reactor before photolysis τ_{res}, and the concentration of H_2O and the flash lamp energy F, which together influence the initial radical concentrations created photolytically.

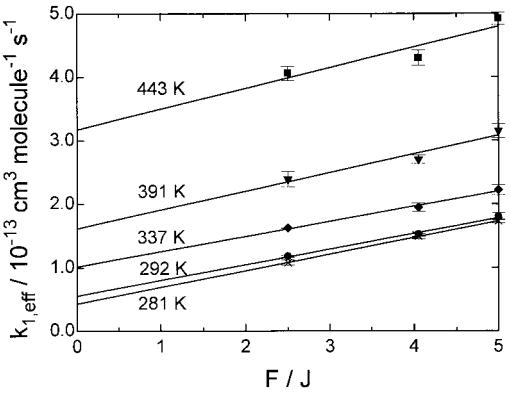

Figure 1. Extrapolations of the effective rate constant for OH + CF_3I, $k_{1,eff}$, to zero radical concentration (flash lamp energy $F = 0$) at each temperature. The points represent weighted means of measurements at the same F, and the error bars represent $\pm 1\sigma$ precision.

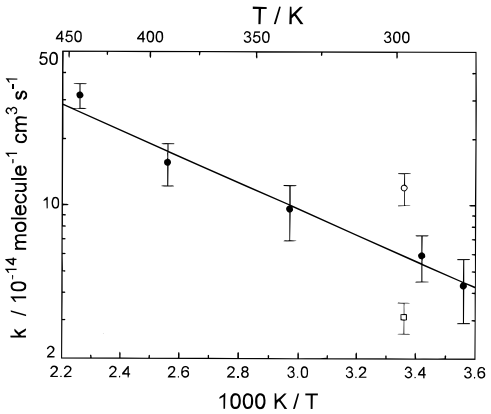

Figure 2. Arrhenius plot for OH + CF_3I: (●) present work; (○) ref 2; (□) ref 3. Error bars represent $\pm 1\sigma$ precision.

3. Experimental Results

Table 1 summarizes 43 measurements of $k_{1,eff}$ at five temperatures. The value of $k_{1,eff}$ was found to be independent of τ_{res}, which indicates that thermal decomposition of CF_3I was negligible. $k_{1,eff}$ was also independent of $[H_2O]$ and thus $[OH]_{t=0}$, which implies that OH did not react significantly with itself or with the reaction products. $k_{1,eff}$ did vary significantly and systematically with the flash energy F which probably reflects secondary chemistry of OH with photolysis fragments of CF_3I. The concentration of these fragments will be approximately proportional to F, so the primary reaction was isolated from interferences by linear extrapolation to zero flash energy, as illustrated in Figure 1. The points in Figure 1 represent weighted means[16] of the $k_{1,eff}$ values at each F. Weighted linear fits[17] to the sets of individual points at each temperature were used to obtain the intercepts and uncertainties listed in Table 1. When $[CF_3I]$ was at the maximum value, typically around 20−40% of the loss of OH was via diffusion. While this is separated from reactive loss of OH via eq 3, the significant contribution by diffusion may contribute to random error in the $k_{1,eff}$ values. The five resulting $k_1(T)$ values are plotted in Arrhenius form in Figure 2 and may be summarized over $T = 280-450$ K as

$$k_1 = (5.8 \pm 2.3) \times 10^{-12} \exp((-11.3 \pm 1.1 \text{ kJ mol}^{-1})/RT) \text{ cm}^3 \text{ molecule}^{-1} \text{ s}^{-1} \quad (4)$$

where the errors are $\pm 1\sigma$ statistical precisions derived from a weighted fit[17] that takes into account errors in both k_1 and T

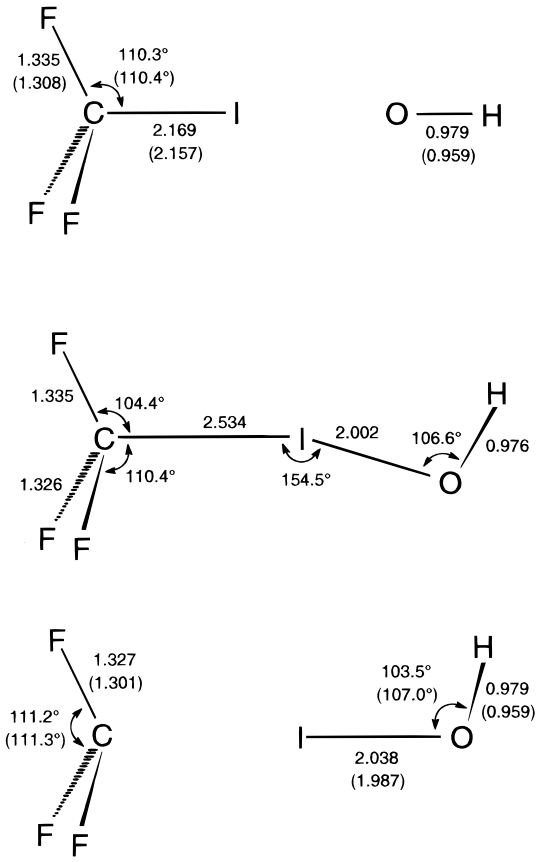

Figure 3. Geometries of reactants, transition state, and products for the OH + CF_3I PES. Angles in degrees and bond lengths in 10^{-10} m. MP2=full/6-31G(d) theory employed, with HF/6-31G(d) values in parentheses. CF_3 and CF_3I have C_{3V} symmetry. Dihedral angles in the TS: ClOH, 81.9°; FCIO (long C−F bond), 175.6°; FCIO (short C−F bonds), +56.7 and −65.9°.

(assumed to be 2%). Consideration of the coupling between the errors in the Arrhenius parameters through the covariance leads to $\pm 1\sigma$ precision estimates for k_1 from 6% at the central temperature of about 350 K to 10% at the extremes. We allow for possible systematic errors of $\pm 1 \times 10^{-14}$ cm^3 molecule^{-1} s^{-1} in the measurements or extrapolations to arrive at an overall 95% confidence interval for k_1 of about ±30% at 280 K improving to ±20% at 450 K.

4. Computational Approach

The general principles of quantitative ab initio molecular orbital theory have been outlined elsewhere.[18,19] The calculations were carried out using the GAUSSIAN 92 and 94 codes[20,21] on SGI Power Challenge, Cray C-916, and Cray YMP-8 computers. Standard atomic basis sets were employed, except for iodine where the basis sets described by Glukhovtsev et al.[22] were used. The geometries of the reagent and product molecules were first optimized at the HF/6-31G(d) level of theory. Scans of the PES at this level indicated no barrier to reaction 1 beyond the endothermicity. Next, the molecular structures were refined at the MP2=full/6-31G(d) level, which includes a partial correction for electron correlation effects applied to all electrons. The optimized geometries are illustrated in Figure 3. At this level a barrier to reaction 1 was located, and its geometry is also shown in Figure 3. Vibrational frequencies were calculated at each of these stationary points on the PES, and they verify that a true TS geometry was obtained, with a single complex frequency that corresponds to motion along the reaction coordinate. The ab initio HF and MP2 frequencies were scaled by 0.8929 and 0.9646,[23] respectively, to approximate the fundamental frequencies (listed in Table 2). As can be seen from Table 2, there is good agreement with the observed frequencies of the reactants and products.[5,29]

Single-point high-level calculations were then carried out at the stationary points to characterize their energy, and these data are listed in Table 3. These are frozen-core, all-electron calculations without effective core potentials.[22] The QCISD-(T)/6-311G(d,p) and MP2/ 6-311+G(3df,2p) results, based on the extension of Gaussian-2 (G2) theory[11] to Br and I by Glukhovtsev et al.,[22] were combined according to the G2(MP2) methodology,[24] where

$$E[\mathrm{G2(MP2)}] = E[\mathrm{QCISD(T)/6\text{-}311G(d,p)}] + E[\mathrm{MP2/6\text{-}311{+}G(3df,2p)}] - E[\mathrm{MP2/6\text{-}311G(d,p)}] + \mathrm{HLC} + \mathrm{ZPE} \quad (5)$$

An empirical higher-level correction is based on the number of α and β valence electrons:[23] $\mathrm{HLC} = -0.00019n_\alpha - 0.00481n_\beta$ hartrees (1 hartree ≈ 2625 kJ mol^{-1}), and E[G2(MP2)] approximates a complete QCISD(T)/6-311+G(3df,2p) calculation. The zero-point vibrational energies (ZPE) are based on MP2 results. Because MP2 frequencies for the TS are available

TABLE 2: Fundamental Vibrational Frequencies ν_0 of Stationary Points on the CF_3I + OH PES (cm^{-1}), Calculated at the HF and MP2 Levels of Theory with the 6-31G(d) Basis Set[a]

CF_3I			OH			CF_3			HOI			TS
HF	MP2	expt[b]	HF	MP2	expt[b]	HF	MP2	expt[b]	HF	MP2	expt[c]	MP2
263 (2)	265 (2)	260 (2)	3570	3607	3570	491 (2)	486 (2)	500 (2)	589	563	575	149 i
278	278	284				677	680	701	1088	1116	1068	24
521 (2)	514 (2)	539 (2)				1086	1086	1090	3659	3577	3626	94
726	718	742				1286 (2)	1271 (2)	1259 (2)				147
1070	1057	1074										171
1243 (2)	1219 (2)	1185 (2)										208
												490
												497
												626
												796
												959
												1091
												1242
												1261
												3608

[a] HF values scaled by 0.8929 and MP2 values scaled by 0.9646. Doubly degenerate modes are indicated by (2). [b] Reference 29. [c] Reference 5.

TABLE 3: G2(MP2) Energies (hartrees) for Stationary Points on the OH + CF_3I PES[a]

species	QCISD(T)/6-311G(d,p)	MP2/6-311+G(3df,2p)	MP2/6-311G(d,p)	HLC	ZPE	G2(MP2)
OH	−75.589 21	−75.617 42	−75.572 76	−0.015 19	0.008 22	−75.640 84
CF_3I	−7253.960 99	−7254.185 89	−7253.924 35	−0.080 00	0.013 78	−7254.288 75
CF_3I−$OH^‡$ TS	−7329.532 85	−7329.798 73	−7329.476 49	−0.095 19	0.025 54	−7329.924 74
HOI	−6992.567 05	−6992.659 70	−6992.543 46	−0.035 00	0.011 97	−6992.706 32
CF_3	−336.967 52	−337.140 09	−336.942 27	−0.060 19	0.012 03	−337.213 50
CF_3IOH adduct	−7329.547 63	−7329.802 25	−7329.491 04	−0.095 19	0.025 03[b]	−7329.929 00

[a] Based on scaled MP2 frequencies and HLC = $-0.00019n_\alpha - 0.00481n_\beta$. 1 hartree ≈ 2625 kJ mol^{-1}. [b] Based on unscaled B3LYP/6-31G(d) frequencies.

TABLE 4: G2 Energies (hartrees) of Ancillary Molecules Used to Estimate $\Delta_f H_0$(HOI)

species	MP4/6-311G(d,p)	ZPE	ΔE(+)	ΔE(2df)	ΔE(QCI)	Δ	E_0(G2)
HOI	−6992.567 72	0.012 15	−0.010 45	−0.091 63	0.000 67	−0.024 83	−6992.716 81
INO	−7046.587 64	0.005 91	−0.007 25	−0.110 20	0.009 43	−0.026 78	−7046.761 53
ICN	−7009.554 09	0.007 84	−0.004 43	−0.095 83	0.004 77	−0.023 82	−7009.705 57
ClCN	−552.276 17	0.008 73	−0.006 71	−0.108 34	0.004 66	−0.006 87	−552.424 69

but HF frequencies are not, our methodology for the PES is a combination of the G2(MP2)[24] and G2(ZPE=MP2)[23] methods. It is noted that calculation of relative energies on the PES cancels the HLC terms. Finally, several small iodine-containing species (HOI, INO, and ICN) and ClCN were characterized with standard G2 theory,[11] which employs ZPE calculated at the HF level and requires additional MP4/6-311G(d,p), MP4/6-311+G(d,p), and MP4/6-311G(2df,p) calculations (Table 4).

5. Discussion

5.1. Kinetics. As shown on Figure 2, the present measurements for k_1 lie midway between the two earlier room temperature determinations. Neither is obviously flawed, although the authors of the discharge−fast flow study[3] (smaller k_1 value) suggested that the laser photolysis−resonance fluorescence study[2] (larger k_1 value) may have been affected by unrecognized secondary chemistry that consumed OH, even though the latter authors sought such effects by variation of the laser intensity but did not observe systematic changes in k_1. The present data yield the first Arrhenius parameters for reaction 1, and the A factor found here, around 10^{-11} cm^3 molecule^{-1} s^{-1}, implies a fairly loose TS and is typical of A factors found for H abstraction reactions by OH from, for example, H_2 or CH_4.[25]

The rate constant at the mean tropospheric temperature of 277 K, estimated from eq 4 to be 4.0×10^{-14} cm^3 molecule^{-1} s^{-1}, is about 5 times that for OH + CH_3CCl_3, and thus the tropospheric lifetime of CF_3I with respect to OH attack is about 0.2 of that of CH_3CCl_3, i.e., about 1.5 years.[26] This result may be compared to a photolytic lifetime of less than 2 days,[27] which indicates that the major loss pathway for CF_3I in the troposphere is via photolysis.

Equation 4 could be extrapolated to combustion temperatures, but frequently it is found that rate expressions of the form $AT^n \exp(-B/T)$ are more realistic than simple Arrhenius expressions over wide temperature ranges. We have estimated $n = 1.5$ for reaction 1 from the vibrational frequencies of the TS and reactants, as outlined by Cohen,[28] and a fit of A and B to our data yields the following rate expression which is proposed for 280−2000 K:

$$k_1 = 2.9 \times 10^{-16} (T/\mathrm{K})^{1.5} \exp(-(960\ \mathrm{K})/T) \quad \mathrm{cm^3\ molecule^{-1}\ s^{-1}} \quad (6)$$

This expression implies $k_1 \approx 10^{-11}$ cm^3 molecule^{-1} s^{-1} at 1500 K so that attack by OH in a flame is rapid, and reaction 1 might therefore be a significant destruction pathway for CF_3I under combustion conditions.

5.2. Product Channels. The products shown for reaction 1, CF_3 + HOI, are those that would be formed by I-atom abstraction by OH. The use of reaction 1 by Monks et al.[6] as a source of HOI demonstrates that HOI production is a significant pathway, but other thermochemically plausible product channels might also be important. An alternative pathway is substitution

$$CF_3I + OH \rightarrow CF_3OH + I \quad (1b)$$

which is exothermic by 252 kJ mol^{-1} at 298 K.[29,30] We were not able to find a TS for this reaction with attack by OH at the opposite side of CF_3I from the C−I bond but did locate a TS for attack at the same face of CF_3I. Thus, if substitution occurs, it appears to preserve the CF_3 group without inversion. The HF/3-21G(d) TS structure has greatly extended C−I and C−O bonds, with lengths of 3.20×10^{-10} and 2.84×10^{-10} m, respectively. The MP4/6-31G(d)//HF/3-21G(d) energy is 202 kJ mol^{-1} above CF_3I + OH, so that channel 1b has too high a barrier to contribute to the observed kinetics. As a check on the reliability of this barrier, the MP4/6-31G(d)//HF/3-21G(d) energy of the TS for reaction 1 was computed and found to be 56 kJ mol^{-1} above CF_3I + OH. As discussed in the next section, this is about 70 kJ mol^{-1} too positive by comparison with more computationally intensive G2(MP2) results. If a similar correction were applied to reaction 1b, its barrier would still be very high, around 130 kJ mol^{-1}.

Ruscic and Berkowitz[31] noted that a possible product channel is

$$CF_3I + OH \rightarrow CF_3O + HI \quad (1c)$$

which is exothermic by 59 kJ mol^{-1} at 298 K.[29,30] We were not able to find a TS for this reaction, although this does not prove that channel 1c does not occur. However, the maximum energy along a linear synchronous path connecting reactants and products at the MP4/6-31G(d) level is 574 kJ mol^{-1} above the reactants. This is an upper limit to the barrier to this reaction if a TS exists, but suggests that channel 1c will be extremely slow.

Wine and McKee and co-workers have investigated adduct formation between halogenated methanes and halogen atoms and hydroxyl radicals. They observed chlorine atom adduct formation at low temperatures (around 250 K) and characterized

adducts computationally using density functional theory.[32] We have analyzed

$$CF_3I + OH\ (+ M) \rightarrow CF_3IOH\ (+ M) \qquad (1d)$$

at the B3LYP/6-31G(d) level of theory and located an adduct with an I−O distance of 2.57×10^{-10} m, bound by 15 kJ mol^{-1} at 0 K (including ZPE). MP2=full/6-31G(d) calculations did not reveal an adduct, and the G2(MP2) energy at the B3LYP/6-31G(d) geometry (Table 3) lies 1.5 kJ mol^{-1} *above* CF_3I + OH. Therefore any adduct is not stable enough to be a significant sink for OH under our experimental conditions.

In summary, channels 1b−d appear to be negligible under our conditions and the dominant products of reaction 1 are CF_3 + HOI, as assumed in the previous experimental kinetic studies.[2,3]

5.3. Experimental thermochemistry and ab Initio PES. The observation that the reaction OH + $I_2 \rightarrow$ I + HOI proceeds at the collision rate at 298 K implies this process cannot be endothermic,[33] and therefore the bond dissociation enthalpy D_{298}(HO−I) must be at least D_{298}(I−I) = 151 kJ mol^{-1}, which combined with the known heats of formation[29] of I and OH implies Δ_fH_{298}(HOI) < −5 kJ mol^{-1}. Jenkin et al. analyzed earlier thermodynamic data[34,35] to obtain −88 and −82 kJ mol^{-1} for this quantity.[33] On the basis of the idea that both reaction 1 and the process HONO + HOI $\rightarrow$ H_2O + INO_2 are "rapid" [*sic*], Jenkin et al.[33] deduced that −77 kJ mol^{-1} ≥ Δ_fH_{298}(HOI) ≥ −102 kJ mol^{-1}. The upper bound rests on the CF_3−I bond strength which Asher et al. recently determined to high precision, $D_{298}(CF_3-I) = 227.2 \pm 1.3$ kJ mol^{-1}.[30] This is more positive than the value of 223 kJ mol^{-1} available to Jenkin et al.[33] and therefore raises the upper bound to Δ_fH_{298}(HOI).

We can use our measured activation energy for reaction 1 to improve the estimates of Δ_fH_{298}(HOI), on the basis of the concept that the enthalpy change for a reaction is equal to the difference between the forward and reverse activation energies:

$$\Delta_rH = E_{a,1} - E_{a,-1} \qquad (7)$$

Using the CF_3−I bond strength at 350 K (the bond strength varies by less than 0.1 kJ mol^{-1} between 298 and 350 K),[29] a temperature that corresponds to the central 1/*T* value of the experiments, it is tempting to assume that the activation energy for the reverse reaction, −1, is given by $E_{a,-1} \geq 0$ and thus D_{350}(HO−I) must be at least 215.9 kJ mol^{-1}. However, the reverse reaction could conceivably have a negative activation energy, perhaps as negative as −5 kJ mol^{-1}, so we more conservatively derive D_{350}(HO−I) ≥ 210.9 kJ mol^{-1} from experimental data alone. This result corresponds to D_0(HO−I) ≥ 205.6 kJ mol^{-1} and contradicts an empirical estimate by Zhang et al.[36] that D_0(HO−I) = 189 ± 2.5 kJ mol^{-1} with an associated Δ_fH_0(HOI) = −42.7 ± 2.5 kJ mol^{-1} (which implies Δ_fH_{298}(HOI) = −46 kJ mol^{-1}). Our result also contradicts Δ_fH_0(HOI) ≈ −36 kJ mol^{-1} estimated empirically by Ruscic and Berkowitz.[31]

Next we consider the PES for reaction −1 in more detail, using the G2(MP2) ab initio results (Table 3). These yield the enthalpy of the TS relative to CF_3 + HOI at 0 K, $E_{0,-1}^{\ddagger} = -13$ kJ mol^{-1}. This negative value is consistent with, but does not prove, that there is no barrier to the reverse of reaction 1. This idea is tested in more detail in Figure 4, where energies obtained at an approximate QCISD/6-311+G(3df,2p) level[37] are plotted as a function of the C−I distance along the reaction coordinate.[38] It may be seen there is no barrier to reaction −1, a result also

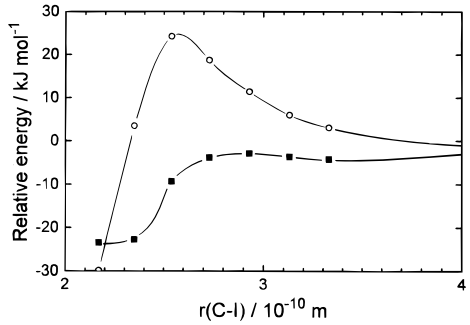

Figure 4. Relative energies along the reaction coordinate for OH + $CF_3I \rightarrow$ HOI + CF_3 computed at (○) MP2=full/6-31G(d) and (■) approximate (see ref 37) QCISD/6-311+G(3df,2p) levels of theory. The energy zero is set at HOI + CF_3, where r(C−I) = ∞. r(C−I) = 2.17×10^{-10} m in the reactants and 2.53×10^{-10} m at the MP2=full/6-31G(d) TS.

TABLE 5: Thermochemistry of HOI and NASA Polynomials

Δ_fH_0(HOI) = −64.9 ± 5.4 kJ mol^{-1}	S_{298} = 255.4 J K^{-1} mol^{-1}
Δ_fH_{298}(HOI) = −69.6 ± 5.4 kJ mol^{-1}	$H_{298} - H_0$ = 10.4 kJ mol^{-1}
$C_{p,298}$ = 38.5 J K^{-1} mol^{-1}	

$$C_p/R = a_1 + a_2T + a_3T^2 + a_4T^3 + a_5T^4$$
$$(\Delta_fH_{298} + H_T - H_{298})/RT = a_1 + a_2T/2 + a_3T^2/3 + a_4T^3/4 + a_5T^4/5 + a_6/T$$
$$S/R = a_1 \ln T + a_2T + a_3T^2/2 + a_4T^3/3 + a_5T^4/4 + a_7$$

	1000−5000 K	50−1000 K
a_1	0.645 448 06 × 10	0.282 512 59 × 10
a_2	−0.149 713 33 × 10^{-2}	0.203 030 59 × 10^{-1}
a_3	0.125 878 52 × 10^{-5}	−0.809 478 44 × 10^{-4}
a_4	−0.325 032 86 × 10^{-9}	0.152 658 80 × 10^{-6}
a_5	0.274 391 48 × 10^{-13}	−0.889 205 86 × 10^{-10}
a_6	−0.932 833 20 × 10^4	−0.965 320 80 × 10^4
a_7	−0.641 009 14 × 10	0.920 611 57 × 10

derived from the low-level HF/6-31G(d) calculations discussed earlier but now confirmed at a much higher level of theory.

This conclusion implies an approximately zero activation energy for −1, and we take $E_{a,-1} = 0 \pm 5$ kJ mol^{-1}. Equation 7 yields Δ_rH for reaction 1 equal to 11.3 ± 5.1 kJ mol^{-1} at 350 K. This reaction enthalpy is related to bond dissociation enthalpies at 350 K via

$$\Delta_rH_{350} = D_{350}(CF_3-I) - D_{350}(HO-I) \qquad (8)$$

The known bond strength for CF_3−I[30] implies D_{350}(HO−I) = 215.9 ± 5.3 kJ mol^{-1}. Since the enthalpies of formation of OH and I are well-known,[29] the HO−I bond strength is employed to estimate Δ_fH_{350}(HOI) = −70.5 ± 5.4 kJ mol^{-1}, where the main source of uncertainty is $E_{a,-1}$ and the contribution from the uncertainties in $E_{a,1}$ and the auxiliary thermochemistry, added in quadrature, is small. The ab initio frequencies (Table 2) are used to calculate the enthalpy function, $H_T - H_0$, which in combination with values for the elements in their reference states[29] yields Δ_fH(HOI) at 298 K of −69.6 ± 5.4 kJ mol^{-1}. The corresponding value at 0 K is −64.9 ± 5.4 kJ mol^{-1}. We have calculated *S*, C_p, and $H_T - H_{298}$ from 50 to 5000 K and fit the results with standard NASA polynomials[39] to obtain thermochemical data in a format suitable for combustion and atmospheric models (see Table 5). The corresponding O−I bond dissociation enthalpy is D_{298}(HO−I) = 215.4 ± 5.4 kJ mol^{-1}. The measured Δ_fH_{298}(IO) = 115.9 ± 5.0 kJ mol^{-1} from Bedjanian et al.[40] yields D_{298}(H−OI) = 403.5 ± 7.4 kJ mol^{-1}, comparable to the C−H bond strength in ethane.[41] Thus, H-abstraction by IO from hydrocarbons is thermodynamically

TABLE 6: G2 Thermochemistry (kJ mol^{-1}) of Working Reactions Used to Calculate $\Delta_f H_0$(HOI)

reaction	$\Delta_r H_0$	$\Delta_f H_0$(HOI)
HOI → H + O + I	623.6	−53.6
HOI + H_2 → H_2O + HI	−150.4	−60.0
HOI + HCl → HOCl + HI	105.0	−55.8
HOI + HI → H_2O + I_2	−140.4	−61.6
HOI + ClCN → ICN + HOCl	71.8	−54.0
HOI + HNO → INO + H_2O	−161.1	−62.7
HOI + H_2S → HSI + H_2O	−103.0	−73.0
HOI + CH_4 → CH_3I + H_2O	−90.2	−56.8

plausible and may need to be taken into account in models of iodine-mediated flame suppression.

5.4. Ab Initio Thermochemistry. The proposed thermochemistry of HOI is in reasonable accord with the earlier experimental limit values outlined above, but there are no measurements with which to compare the new result. The recent implementation of G2 theory for iodine compounds by Glukhovtsev et al.[22] enables an independent check of $\Delta_f H_0$(HOI). The G2 energy of HOI (Table 4), together with values for the atoms,[11,22] yields ΔH_0 for atomization. However, this process involves considerable changes in the electronic structures of the atoms which might not be well accounted for, so we have also considered seven other processes, listed in Table 6, which relate the unknown $\Delta_f H_0$(HOI) to known values for other small molecules. The computed $\Delta_r H_0$ values derived from the G2 energies[11,42] (see Table 4) for these reactions together with experimental values for $\Delta_f H_0$ of H, O, I, H_2O, HI, H_2S, ClCN, ICN, HOCl, HCl,[29] HNO,[43] INO,[44] CH_3I[45] and HSI,[46] lead to the $\Delta_f H_0$(HOI) values listed in Table 6. The mean of the eight values is −60 kJ mol^{-1} (standard deviation 6 kJ mol^{-1}) which is in good accord with our new experimental value of −65 ± 5 kJ mol^{-1}.

This computed $\Delta_f H_0$(HOI) is 15 kJ mol^{-1} more negative than the value recently obtained by Glukhovtsev et al.[47] also using G2 theory. The difference appears to arise about equally from their use of effective core potentials, by contrast to the all-electron basis sets employed here, and from their consideration of only the first working reaction of Table 6. This atomization step gives the most positive $\Delta_f H_0$(HOI) of all the processes analyzed, but we consider it the least reliable. Very recently Hassanzadeh and Irikura[48] used different working reactions and CCSD(T) theory to obtain $\Delta_f H$(HOI) at 0 and 298 K of −55.2 and −59.9 ± 6.9 kJ mol^{-1}, respectively, in good accord with the computed and experimentally based values presented here.

6. Conclusions

The temperature dependence of the rate constant for the reaction OH + CF_3I has been measured, and ab initio analysis suggests the dominant products are CF_3 and HOI. The measured Arrhenius parameters, together with an estimated activation energy $E_{a,-1}$ for the reverse reaction supported by an ab initio analysis of the potential energy surface, yield the heat of formation of HOI. The main uncertainty in the present work lies in $E_{a,-1}$. This experimental value for $\Delta_f H$(HOI) is confirmed by a direct computational estimate and is more negative than recent empirical values. The temperature dependence of the rate constant suggests that OH attack is a minor contributor to the loss of CF_3I in the troposphere but a potentially significant channel for CF_3I destruction under combustion conditions.

Acknowledgment. We thank Drs. M. P. McGrath and L. Radom for valuable advice on G2 calculations for I-containing species, together with Drs. K. K. Irikura and L. J. Stief for preprints of unpublished work. This work was supported by the Air Force Office of Scientific Research, the R. A. Welch Foundation (Grant B-1174), and the UNT Faculty Research Fund. Cray computer time was provided by the Department of Defense High Performance Computing Center, CEWES, Vicksburg, MS.

References and Notes

(1) Tapscott, R. E.; Skaggs, S. R.; Dierdorf, D. in *Halon Replacements*; Miziolek, A. W., Tsang, W., Eds.; ACS Symposium Series 611; American Chemical Society: Washington, D.C., 1995.

(2) Garraway, J.; Donovan, R. *J. Chem. Soc., Chem. Commun.* **1979,** 1108.

(3) Brown, A. C.; Canosa-Mas, C. E.; Wayne, R. P. *Atmos. Environ.* **1990**, *24A*, 361.

(4) Wang, J. J.; Smith, D. J.; Grice, R. *J. Phys. Chem.* **1996**, *100*, 6620.

(5) Klaassen, J. J.; Lindner, J.; Leone, S. R. *J. Chem. Phys.* **1996**, *104*, 7403.

(6) Monks, P. S.; Stief, L. J.; Tardy, D. C.; Liebman, J. F.; Zhang, Z.; Kuo, S.-C.; Klemm, R. B. *J. Phys. Chem.* **1995**, *99*, 16566.

(7) Loomis, R. A.; Klaassen, J. J.; Lindner, J.; Christopher, P. G.; Leone, S. R. *J. Chem. Phys.* **1997**, *106*, 3934.

(8) Frey, J. G. In *Photodissociation Dynamics*; Balint-Kurti, G. G., Law, M. M., Eds.; Collaborative Computational Project on Heavy Particle Dynamics; Daresbury Laboratory: Warrington, U.K., 1994; p 22.

(9) Babushok, V.; Noto, T.; Burgess, D. R. F.; Hamins, A.; Tsang, W. *Combust. Flame* **1996**, *107*, 351.

(10) Solomon, S.; Garcia, R. R.; Ravishankara, A. R. *J. Geophys. Res.* **1994**, *99*, 20, 491.

(11) Curtiss, L. A.; Raghavachari, K.; Trucks, G. W.; Pople, J. A. *J. Chem. Phys.* **1991**, *94*, 7221.

(12) Shi, Y.; Marshall, P. *J. Phys. Chem.* **1991**, *95*, 1654.

(13) Ding, L.; Marshall, P. *J. Phys. Chem.* **1992**, *96*, 2197.

(14) Yuan, W.-J.; Misra, A.; Hommel, E.; Goumri, A.; Marshall, P. To be published.

(15) (a) Marshall, P. *Comput. Chem.* **1987**, *11*, 219. (b) Marshall, P. *Comput. Chem.* **1989**, *13*, 103.

(16) Bevington, P. R. *Data Reduction and Error Analysis for the Physical Sciences*; McGraw-Hill: New York, 1969: p 88.

(17) Irvin, J. A.; Quickenden, T. I. *J. Chem. Educ.* **1983**, *60*, 711.

(18) Hehre, W. J.; Radom, L.; Schleyer, P. v. R.; Pople, J. A. *Ab Initio Molecular Orbital Theory*; Wiley: New York, 1986.

(19) Foresman, J. B.; Frisch, Æ. *Exploring Chemistry with Electronic Structure Methods*; Gaussian: Pittsburgh, PA, 1993.

(20) Frisch, M. J.; Trucks, G. W.; Head-Gordon, M.; Gill, P. M. W.; Wong, M. W.; Foresman, J. B.; Johnson, B. G.; Schlegel, H. B.; Robb, M. A.; Replogle, E. S.; Gomperts, R.; Andres, J. L.; Raghavachari, K.; Binkley, J. S.; Gonzalez, C.; Martin, R. L.; Fox, D. J.; DeFrees, D. J.; Baker, J.; Stewart, J. J. P.; Pople, J. A. *GAUSSIAN 92*; Gaussian: Pittsburgh, PA, 1992.

(21) Frisch, M. J.; Trucks, G. W.; Schlegel, H. B.; Gill, P. M. W.; Johnson, B. G.; Robb, M. A.; Cheeseman, J. R.; Keith, T.; Petersson, G. A.; Montgomery, J. A.; Raghavachari, K.; Al-Laham, M. A.; Zakrzewski, V. G.; Ortiz, J. V.; Foresman, J. B.; Peng, C. Y.; Ayala, P. Y.; Chen, W.; Wong, M. W.; Andres, J. L.; Replogle, E. S.; Gomperts, R.; Martin, R. L.; Fox, D. J.; Binkley, J. S.; Defrees, D. J.; Baker, J.; Stewart, J. P.; Head-Gordon, M.; Gonzalez, C.; Pople, J. A. *GAUSSIAN 94*; Gaussian: Pittsburgh, PA, 1995.

(22) Glukhovtsev, M. N.; Pross, A.; McGrath, M. P.; Radom, L. *J. Chem. Phys.* **1995**, *103*, 1878.

(23) Curtiss, L. A.; Raghavachari, K.; Pople, J. A. *J. Chem. Phys.* **1995**, *103*, 4192.

(24) Curtiss, L. A.; Raghavachari, K.; Pople, J. A. *J. Chem. Phys.* **1993**, *98*, 1293.

(25) Mallard, W. G.; Westley, F.; Herron, J. T.; Hampson, R. F. *NIST Chemical Kinetics Database*, Ver. 6.0; NIST Standard Reference Data; National Institute of Standards and Technology: Gaithersburg, MD, 1994.

(26) Chang, D. T.; Gurney, K. R.; Ko, M. K. W.; Kolb, C. E.; Nelson, D. D., Jr.; Rodriguez, J. M.; Weisenstein, D. K. In *Chemicals in the Atmosphere*; Chang, D. T., Sze, N. D., Eds.; Atmospheric and Environmental Research: Cambridge, MA, 1992.

(27) Solomon, S.; Burkholder, J. B.; Ravishankara, A. R.; Garcia, R. R. *J. Geophys. Res.* **1994**, *99*, 20929.

(28) Cohen, N. *Int. J. Chem. Kinet.* **1989**, *21*, 909.

(29) Chase, M. W., Jr.; Davies, C. A.; Downey, J. R., Jr.; Frurip, D. J.; McDonald, R. A.; Syverud, A. N. JANAF Thermochemical Tables, 3rd ed. *J. Phys. Chem. Ref. Data* **1985**, *14*, Suppl. 1.

(30) Asher, R. L.; Appelman, E. H.; Tilson, J. L.; Litorja, M.; Berkowitz, J.; Ruscic, B. *J. Chem. Phys.* **1997**, *106*, 9111.

(31) Ruscic, B.; Berkowitz, J. *J. Chem. Phys.* **1994**, *101*, 7795.
(32) Piety, C. A.; Nicovich, J. M.; Ayhems, Y. V.; Estupinan, E.; Soller, R.; McKee, M. L.; Wine, P. H. *14th International Symposium on Gas Kinetics*, paper D6; Leeds, 1996.
(33) Jenkin, M. E.; Clemitshaw, K. C.; Cox, R. A. *J. Chem. Soc., Faraday Trans. 2* **1984**, *80*, 1633.
(34) Gelles, E. *Trans. Faraday Soc.* **1951**, *47*, 1158.
(35) Garisto, F. *Thermochim. Acta* **1983**, *63*, 251.
(36) Zhang, Z.; Monks, P. S.; Stief, L. J.; Liebman, J. F.; Huie, R. E.; Kuo, S.-C.; Klemm, R. B. *J. Phys. Chem.* **1996**, *100*, 63.
(37) Derived as in eq 5 except that the triples contribution to the QCI energy and the ZPE were neglected.
(38) The reaction coordinate was obtained by fixing the C−I distance and reoptimizing the structure. When the C−I distance exceeded 2.7×10^{-10} m, the geometry had relaxed essentially to that of $CF_3 + HOI$, so for subsequent points only the C−I distance was varied, with the rest of the structure held constant.
(39) Burcat, A. In *Combustion Chemistry*; Gardiner, W. C., Jr., Ed.; Springer-Verlag: New York, 1984; Chapter 8 and Appendix A.
(40) Bedjanian, Y.; Le Bras, G.; Poulet, G. *J. Phys. Chem. A* **1997**, *101*, 4088.
(41) Berkowitz, J.; Ellison, G. B.; Gutman, D. *J. Phys. Chem.* **1994**, *98*, 2744.
(42) Hommel, E.; Misra, A.; Marshall, P. To be published.
(43) Anderson, W. R. Personal communication, 1996.
(44) Hippler, H.; Luther, K.; Teitelbaum, H.; Troe, J. *Int. J. Chem. Kinet.* **1977**, *9*, 917.
(45) Lias, S. G.; Bartmess, J. E.; Liebman, J. F.; Holmes, J. L.; Levin, R. D.; Mallard, W. G. Gas-Phase Ion and Neutral Thermochemistry. *J. Phys. Chem. Ref. Data* **1988**, *17*, Suppl. 1.
(46) Hwang, R. J.; Benson, S. W. *J. Am. Chem. Soc.* **1979**, *101*, 2615.
(47) Glukhovtsev, M. N.; Pross, A.; Radom, L. *J. Phys. Chem.* **1996**, *100*, 3498.
(48) Hassanzadeh, P.; Irikura, K. K. *J. Phys. Chem. A* **1997**, *101*, 1580.